Buckling of perforated discs

COSTICĂ ATANASIU[1,2*], ŞTEFAN SOROHAN[1]

[1]*Strength of Materials Department, Politehnica University of Bucharest,*
[2]*The Academy of Technical Sciences in Romania*

Abstract. The paper presents the results obtained regarding the stability of discs perforated by two, four and 96 circular holes. Circular discs are subjected to two types of loadings: diametrical compression by concentrated forces and radial compression produced by an equivalent uniformly distributed load on the contour of the disks. The influence of the radius of the holes, the distance between the holes and the way of applying the loads, on the value of the critical buckling load is investigated. The results obtained by the finite element method are compared with those obtained in the case of non-perforated disks with the same support conditions and required with the same loads. At the same time, the forms of loss of stability and the values of the buckling safety coefficients for the analyzed disks are determined.

Key words: buckling safety factor, critical buckling load, finite element method, perforated disk, stability

1. Introduction

Using of steels and their alloys in thin engineering structures has made the issue of their elastic stability of great importance. The use of steel resulted in slender constructions with sub-assemblies subject to compression. This is the case of thin plates that can fail due to large deformations and/or loss of elastic stability without exceeding the allowable stresses. A particular case is also the problem of compressed discs which can fail through lateral instabilities.

The first investigations on the loss of stability in bars were carried out in by Euler [1], [2]. In his studies he admitted that the bar, for the four fundamental cases of clamping at the ends, buckles. In this situation, starting from the differential equation of the deformed beam axis and the boundary conditions in the support systems, Euler finds the expression for the minimum force that would produce

---

* Correspondence address: atanasiucostica@yahoo.com

extremely large deformations, tending to infinity. This value of the force was called the critical buckling load.

Timoshenko [3], [4] studies the elastic stability of thin circular plates of radius *R* supported or clamped on the contour and loaded in the middle plane with loads uniformly distributed all around. Like Euler in the case of bars, Timoshenko admits that the plate buckles under the action of compression forces in the median plane and that the deformed surface is axially symmetric. From the differential equation of the deformed surface, which has as a solution a sum of Bessel functions of the first order of the first and second kinds, obtain the expression of the critical buckling distributed load (N/m) for the clamped plate on the contour in the form:

$$\left(N_r\right)_{cr} = 14.68 \frac{D}{R^2},\tag{1}$$

rigidity of the plate, and *t* is the constant thickness of plate.

In a similar way, he solves the buckling problem of thin circular plates simply supported on the contour and loaded with uniformly distributed compressive forces in the middle plane on the plate contour, obtaining for the critical buckling load the expression

$$\left(N_r\right)_{cr} = 4.20 \frac{D}{R^2},\tag{2}$$

so a critical force 14.68/4.2 = 3.5 times lower than in the case of the clamped plate on the contour.

Timoshenko also studies the stability of a circular plate with a central hole for which he derives the expression for the critical buckling load. This depends on the radius of the hole *r* and the radius of circular plate *R* as well as the stiffness of the plate. The general formula can be written as

$$\left(N_r\right)_{cr} = k \frac{D}{R^2},\tag{3}$$

where $k\left(\dfrac{r}{R}\right)$ is given in Fig. 1 for clamped and simply supported external edges.

Another method for determining the critical buckling force [4] assumes that the plate buckles slightly under midplane forces and determines the amount of forces to hold the plate in this shape. By solving the differential equation of the deformed plate and setting the boundary conditions, the values of the forces that produced the buckling are determined. The lowest value represents the critical buckling load.

For more complex geometries as circular plates with more holes and loads which are not symmetric, it is very difficult to obtain an analytical solution of critical forces. The approximate finite element method is a good alternative.

Next we review the classical eigenbuckling problem which may be used in a Finite Element Analysis (FEA) of similar applications.
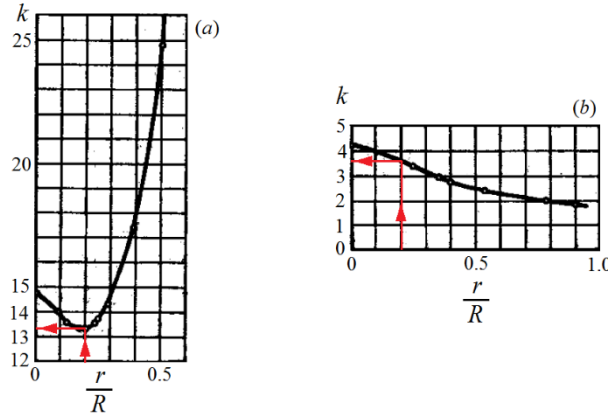
Fig. 1. Variation of coefficient *k* in relation (3) for a circular plate with a central hole.
(a) clamped external edges; (b) simply supported external edges.

2. Eigenbuckling problem in FEA

As analytically, the equilibrium equation in FEA must be written in deformed configuration [5, 6]. The linear elastic stiffness matrix [*K*], used in static analyses is obtained in small displacement conditions. It is necessary to correct the total stiffness matrix with the geometric stiffness matrix [K_σ] which is a function of the stress state. [K_σ] is initially unknown. Equilibrium in a deformed state which represents an instable configuration results as the following nonlinear global equilibrium equation of the model:

$$\left([K] + [K_\sigma] \right) \{U\} = \{F\}, \tag{4}$$

where $\{U\}$ is the displacement vector and $\{F\}$ the external force vector.
In practice, the procedure for obtaining the critical forces (bifurcation points) is as follows:
1. A reference load $\{F_{ref}\}$ is considered. A static analysis is performed, using the equation $[K]\{U_{ref}\} = \{F_{ref}\}$, in order to obtain the membrane stresses and then the matrix $[K_{\sigma, ref}]$. A simplifying hypothesis of load variation is made in the form:

$$\{F\} = \lambda \{F_{ref}\}, \tag{5}$$

where λ is a scalar (the forces increase proportionally). Since the initial calculus is linear, it results:

$$[K_\sigma] = \lambda [K_{\sigma,ref}] \tag{6}$$

2. A bifurcation point correspond to two equilibrium states $\{U\}$ and $\{U + dU\}$ for the loading case defined by $\lambda_{cr}\{F_{ref}\}$. Thus, one can write:

$$\left([K] + \lambda_{cr} [K_{\sigma,ref}] \right) \{U\} = \left([K] + \lambda_{cr} [K_{\sigma,ref}] \right) \left(\{U\} + \{dU\} \right) = \lambda_{cr} \{F_{ref}\}. \tag{7}$$

From the above relation, it results:

$$\left([K] + \lambda_{cr} [K_{\sigma,ref}] \right) \{dU\} = \{0\}. \tag{8}$$

This is the equation of an eigenvalue problem that can be rewritten as:

$$[K]\{dU\} = -\lambda_{cr}\left[K_{\sigma,ref}\right]\{dU\}. \tag{9}$$

From (9), one can obtain *the safety coefficients for loss of stability* $c_{cr} = -\lambda_{cr}$ for the reference loading, that means:

$$\{F_{cr}\} = c_{cr}\left\{F_{ref}\right\}. \tag{10}$$

The mode shapes of loss of stability with respect to the equilibrium position $\{U\}$ are given by the vectors $\{dU_{cr}\}$, associated to the coefficients $c_{cr} = -\lambda_{cr}$. Because this type of analysis is adequate for structures with small displacements, the modal shapes of loss of stability are referred to the initial, non-deformed shape.
The smallest eigenvalue (or some of the smaller) are of most interest in practice. Equation (9) is sometimes written in finite element codes in simplified form as

$$[K]\{\phi\} = \lambda[K_{\sigma}]\{\phi\}. \tag{11}$$

3. Partial validation of results obtained using FEA

For a circular plate and a circular with a central hole which are axial symmetrical loaded on external edges with radial uniform distributed load N_r the critical load can be found analytically using relations (1) - (3) and Fig. 1. Next, for particular cases of geometry, the same problems were solved using Ansys.
Considering $r/R = 0.2$, from Fig. 1 results $k = 13.3$ for the case of clamped plate and $k = 3.60$ for the case of simply supported plate. Critical loads $(N_r)_{cr}$ for the folowing input data: $E = 3400$ MPa; $v = 0.3$, $R = 150$ mm; $t = 10$ mm and $r = 0.2R = 30$ mm are presented in Table 1.

Table 1. Critical loads $(N_r)_{cr}$ in (N/mm) obtained analytically and using FEA

Boundary conditions	Clamped edges			Simply supported edges		
Case	Analytic	FEA	Error [%]	Analytic	FEA	Error [%]
Circular plate	203.1	199.4	1.82	58.12	57.78	0.59
Circular plate with a hole in the center	184.05	185.49	-0.78	49.82	48.71	1.41

In Fig. 2 is presented the finite element model for the circular plate with a hole in the center. The reference load was considered as 1 N/m and in this case the smallest eigenvalue corresponds to the critical load. For meshing, the quadrilateral eight-nodded shell element (Shell 281) was considered.
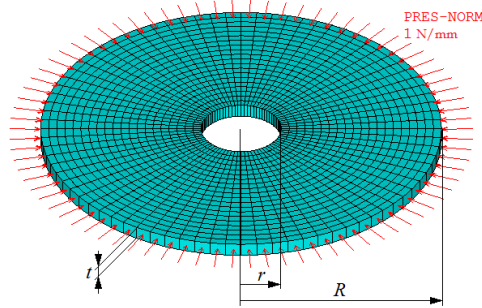
Fig. 2. Geometry, mesh and load of a circular plate with a hole in the center.

The principal stress distributions obtained for reference load in Fig. 2 ($N_r = 1$ N/m) are presented in Fig. 3 in cylindrical system of coordinates (RSYS = 1). One can observe that the stress distributions correspond to boundary conditions, i.e. the radial stresses are between 0.1 MPa (because $t = 10$ mm) on the external contour and zero (0.001 MPa due to small errors in finite element model, the mesh is not fine enough) on the internal contour.

The smallest load factors and modes of instabilities are presented in Fig. 4. For the case of circular plate without central hole the modes are similar and are not presented here.
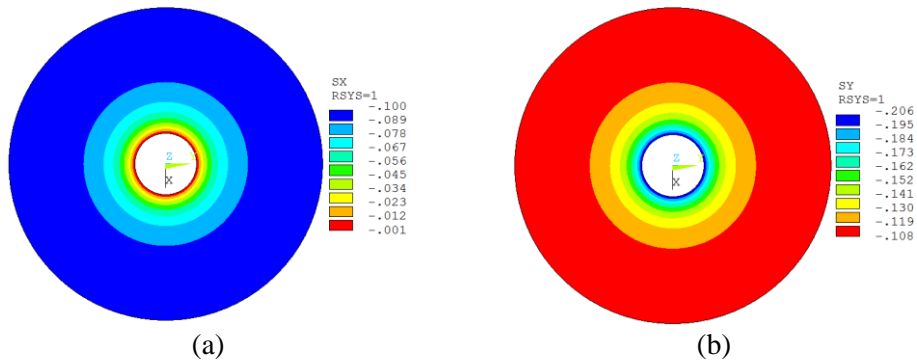

(a)   (b)
Fig. 3. Principal stress distribution for the radial load in Fig. 2.
(a) Radial; (b) Circumferential.
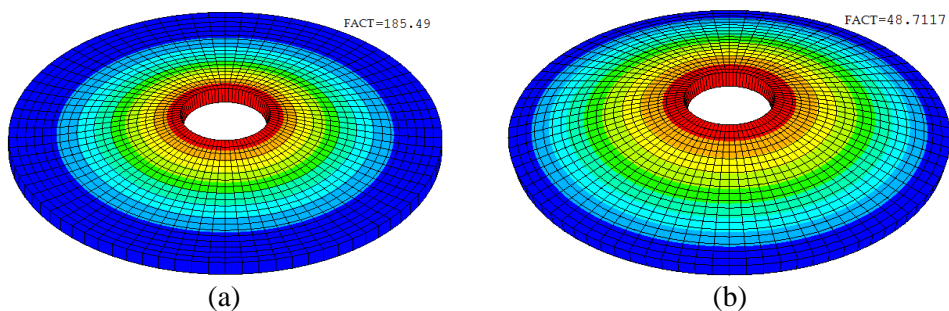

(a)   (b)
Fig. 4. Instability modes for model in Fig. 2 obtained using FEA. (a) Clamped edges; (b) Simply supported edges. Here "FACT" represents exactly critical radial load in N/m.

From Table 1, one can see that the error between analytically and FEA results are small enough to consider that the finite element type used in modeling is adequate and it may be used for more complex simulations.

4. FEA results and discussion for complex perforated discs

Perforated circular discs represent sub-assemblies frequently found in the construction of motor vehicles, agricultural machines, and machinery in the process industry. Perforated discs subjected to diametrical compression may have geometric and loading symmetry. The discs under study differ from those studied so far both in geometry and in the way of applying of the compression force. The discs are perforated with two, four or 96 holes and the compression force is applied to a very small area (Fig. 5).

The research carried out refers to circular discs with radius $R = 150$ mm and constant thickness $t = 10$ mm, perforated by with two, four or 96 circular holes with radii r in the range 1 to maximum 50 mm (1, 2, 5, 10, 20, 30, 40, 50 mm. The two and four holes respectively (Fig. 5,b,c) are arranged on a circle with radius $R_1 = 75$ mm, on the horizontal diameter respectively on the horizontal diameter and on the vertical diameter of the perforated discs. The centers of the 96 holes (Fig. 4,d) are arranged in a grid of squares with a side of $a = 24$ mm. The discs are made of plexiglass with the elastic characteristics: Young's modulus $E = 3400$ MPa and Poisson's ratio $v = 0.3$. Perforated discs subjected to diametrical compression present both geometric and loading symmetry.
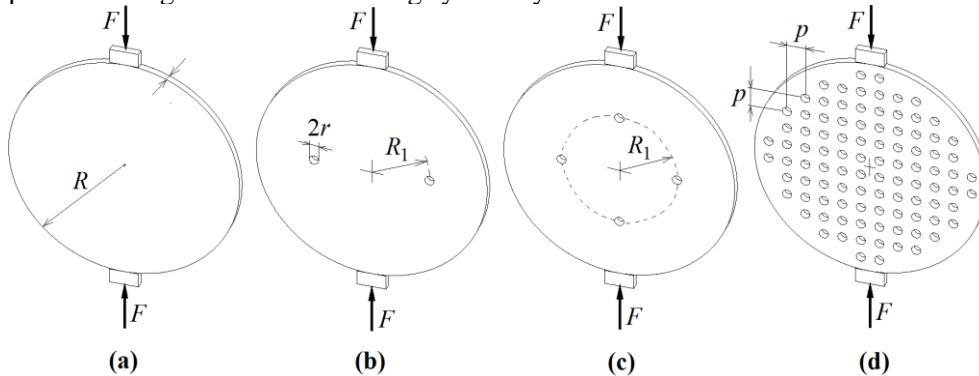

Fig. 5. Researched discs for lateral instabilities.

The static analysis of the distribution of displacements and stresses in the discs, as well as the investigation of their stability, was carried out by the finite element method, using Shell281 finite element type in software Ansys [5], [6]. The discretization in finite elements was performed for the four types of discs studied: non-perforated disc, disc perforated by two, four or 96 holes. When discretizing the non-perforated disc, it was considered that it should be done in such a way that by extracting some areas, the disc perforated by two, four and 96 holes with the expected values of the radii would result. At the same time, it was considered that

in the vicinity of the holes with a very small radius and in the area of contact of the disk with the block through which the compression force is applied, a fine refinement of the discretization should be done. In the area of transmission of the compression force (around of 6 - 8 mm), a parabolic distribution of the pressure with the equivalent force *F* was imposed.

In Fig. 6 are presented the discretizations and boundary conditions for two holes of the analyzed models for a particular radius *r* of 10 mm subjected to compression by the force *F* = 1000 N. The load was considered very close to real condition using the relation below in global coordinates (see Fig. 6,a)

$$p(x) = p_0 \left[1 - \left(\frac{x}{c} \right)^2 \right],$$ (12)

where $p_0 = \dfrac{3}{4} \dfrac{F}{c}$ and *c* was obtained from a previous static nonlinear analysis [7], and it is around of 3 - 4 mm for *F* = 1000 N. For example for the case of two holes *c* = 3.85 mm. Because the mesh size around the applied pressure is around of 0.2 mm (finite), the applied force was checked using numerical integration of the applied pressure over the elements
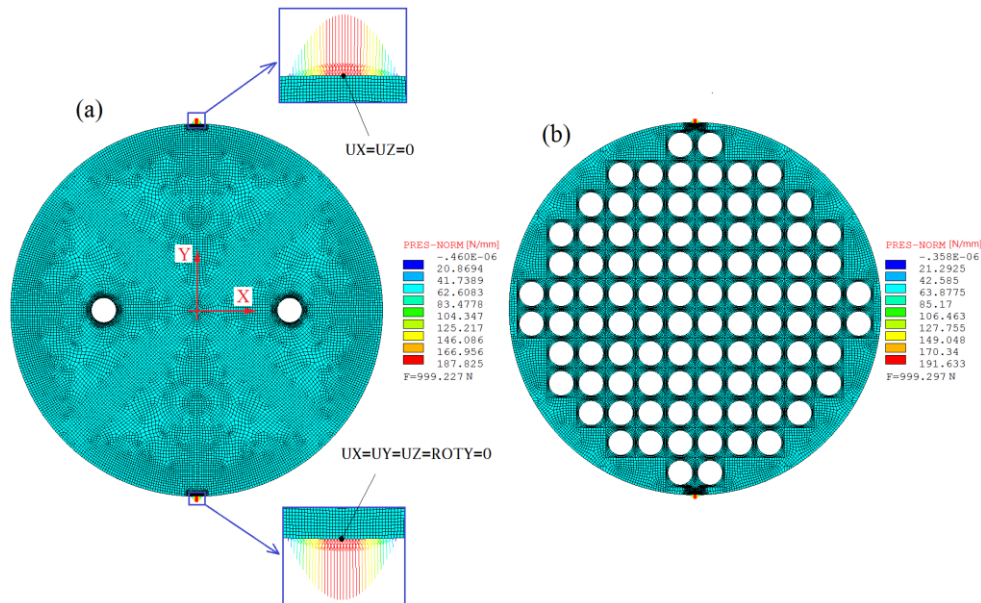
$$F = \int_{-c}^{c} p(x) dx .$$ (13)

Fig. 6. Discretization and boundary conditions when load was applied as parabolic distributed pressure. (a) Disk with two holes; (b) Disk with 96 holes.

The analysis was considered also for the same fixed DOFs and rigid region condition (constraint equations) for the top and bottom nodes for the same distance 2*c* (Fig. 7) and it was obtained practically the same values for the load factors. As

one can see in Fig. 7, the distributed load results nonrealistic and stress distribution in the rigid region zone is locally perturbed but it does not have influence in the eigenvalue problem.
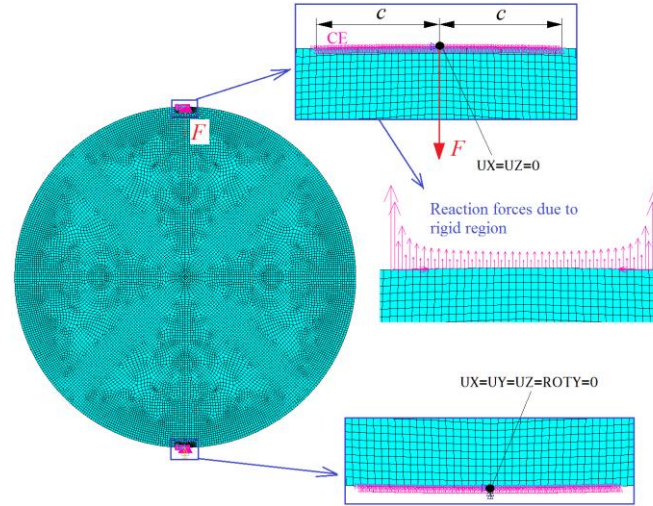

Fig. 7. Discretization and boundary conditions when load was applied on a rigid region for the case of disk without holes.

The research was carried out for several variants of the clamping of the discs at the ends and the way of transmission of the diametrical compression force s discussed. The discs were considered hinged at the ends (case 1) or embedded at one end and free at the other end (case 2).

In the present work, the results obtained only for one of the studied cases are presented extensively (case 1). The verification of the performed modeling was done by calculating the stresses in the center of the non-perforated disc, which were obtained by the finite element method in reference [7], i.e. $\sigma_1 = 2.12$MPa and $\sigma_3 = -6.36$ MPa compared to $\sigma_1 = 2.12$ MPa and $\sigma_3 = -6.37$MPa, results from the analytical calculation. This confirms the assessment that the schematizations and discretizations used for the applied loads and the disc geometry were very close to the real situation of the studied problem.

The results regarding the finite element analysis of stress distribution in perforated discs were analyzed in the paper [7]. The investigation of the elastic stability of the discs was carried out with the software Ansys 19 , which makes the same assumptions as in the papers [3], [4], but solves the resulting differential equations using the finite element method. The values of the forces that produce the buckling of the discs are thus obtained. The ratio between the critical buckling load and the compressive force acting on the discs, according to (10) is the buckling safety factor

$$c = \frac{F_{cr}}{F} \,. \tag{14}$$

The software Ansys renders the number of loss of stability shapes required for each perforated disc corresponding to the forces that produce them but only the lowest value of the force represents the critical buckling load. From the multitude of cases studied, they are shown in Fig. 8 and in Table 2 when the holes had a radius of 10 mm.
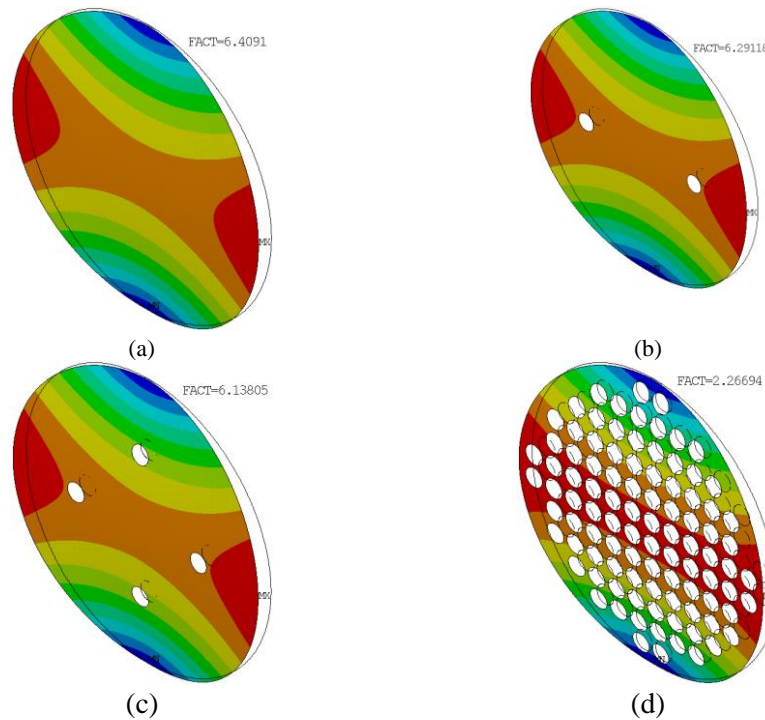

(a)   (b)

(c)   (d)

Fig. 8. Fundamental modes of instability for models in Fig. 5 obtained using FEA for *r* = 10 mm and *F* = 1000 N.

From the Table 2 one can see that critical buckling load decreases with increasing the number of holes and reducing the area of the discs. If for the full disc the critical buckling load is $F_{cr} = 6409$ N, for the disk with two holes this force decreases to $F_{cr} = 6291$ N, for the same disc with four holes it decreases to $F_{cr} = 6138$ N and for the disc with 96 holes it decreases to $F_{cr} = 2266.9$ N, that means a reduction of the critical buckling load for the 96-hole disc by 2.78 times that of the two-hole disc and 2.83 times that of the non-perforated disc.

Table 2. Stability calculation results for the discs

Disc	Disc area [mm^2]	Critical load [N]	Safety factor [-]
Full	70685	6409	6.4091
With 2 holes	70057	6291	6.2912
With 4 holes	69429	6138	6.138
With 96 holes	40526	2266.9	2.2669

Table 3 shows the results of the stability calculations for the disc perforated by four holes with radii *r* between 1 mm and 50 mm. It is found that increasing the radius of the holes leads to a decrease in the area of the disc and the critical buckling load. If the radius of the holes is *r* = 1 mm, the critical buckling load is F_{cr} = 6405 N compared to F_{cr} = 6409 N for the non-perforated plate; at *r* = 50 mm the critical load of buckling is F_{cr} = 1882 N, so a 3.4-fold reduction in the force that causes the loss of disc stability.

Table 3. Stability calculation results for the perforated disc by four holes

Hole radius [mm]	Disc area [mm²]	Critical load [N]	Safety factor [-]
1	70673	6405	6.405
2	70635	6395	6.395
5	70371	6333	6.333
10	69429	6138	6.138
20	65659	5462	5.462
30	59376	4518	4.518
40	50579	3378	3.378
50	39269	1882	1.882

The discs show symmetry not only geometrically and loading, but also in terms of rigidity and grip. For these reasons, regardless of the number of holes, the disks retain their form of loss of stability but which have maximum displacements which are produced by forces of different places along the horizontal diameter. The mode of fastening at the ends of the discs has a main role in determining the buckling shapes. For example in Fig. 9 is presented the fundamental buckling mode of the disc with four holes and *r* = 20 mm bonded in the lower part over a distance 2*c* = 6 mm (see Fig. 7 in which UX=UY=UZ=ROTX=ROTY=ROTZ=0) and free in the rest loaded in compression with the same force *F* = 1000 N.

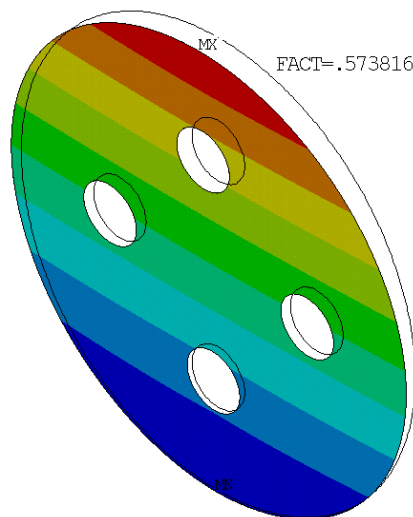Fig. 9. Buckling form for a fixed disc at the lower part and free at the upper part
(*r* = 20 mm)

Following the research undertaken in the paper on the elastic stability of circular discs perforated by two, four or 96 circular holes, subjected to diametrical compression by concentrated forces considered distributed according to a parabolic law in the contact area, some conclusions can be drawn regarding the factors that influence the value of the critical forces at which the discs lose their stability. One of these factors is the stiffness of the disc, finding that when the effective area of the disc decreases, the value of the critical buckling force also decreases. Thus, for the disc with 96 holes with the radius r=10mm, the critical buckling force is almost three times lower than for the solid disc. At the same time, for the disc perforated by the same number of holes, the critical buckling force decreases with the increase of the radius of the holes. For example, for the disc with four holes with their radius r=1mm F_{cr}=6405N and for the same disc with holes having the radius r=50mm the critical buckling force F_{cr}=1882N, i.e. a 3.4 times reduction of the force that causes the loss of disc stability. The way the disc is clamped at the place of transmission of the compressive load influences the value of the critical buckling force. Thus, for a disk considered articulated-articulated, the force of loss of stability is much higher than in the case of the same disk, with the same number of holes, of the same radius but considered recessed-free end. And the way of applying the load can influence the value the critical buckling load. A compression load transmission through an elastic element with a distribution considered according to a parabolic law is more favourable than force transmission through a rigid element and a distribution considered uniform. In the first situation of load transmission, the value of the force at which the disc loses its stability is higher than in the second case If a comparison is made between the disc perforated through four holes with a radius of r=20mm in the variant in which it is elastically clamped at the ends and subjected to compression and the same disc which is embedded at one end and is free at the other end, it can be said that in the variant articulated-articulated at the ends, the critical buckling is produced by the force F=5462 N and in the embedded-free-end version the buckling is produced by the force F=146.8 N. In this case the stress in the center of the disk corresponding to the critical buckling force is σ_{cr} =0.22MPa compared to the stress corresponding to this compression force σ=0.568MPa. Buckling for this type of grip occurs at a compressive stress in the center of the disc 2.58 times lower than in the case of simple compression.

 Finite element analysis allows the use of a variety of assumptions and schematizations that bring the numerically analyzed problem closer to the real problem.

5. The stability of perforated discs loaded with uniformly distributed load on the contour

The stability analysis was also performed for the case where the concentrated radial force F=1000N is uniformly distributed on the circumference of the discs of radius R=150mm, as a uniform pressure.

In this situation the value of the load force distributed on the contour is

$$p_\ell = \frac{F}{2\pi R} = 1.061 \text{ N/mm.}$$

To eliminate rigid body displacements, discs were considered articulated on the vertical diameter. On the outer contour of the discs only use movements are blocked. In the stability analysis, the loss of stability modes can be symmetric/antisymmetric, which is why full disc models were used. . After the discretization of the perforated discs with two, four and 96 holes with a radius between 1 and 50 mm and their loading with the uniform radial load p (fig.10), the stability in the discs was analyzed.

(a)   (b)
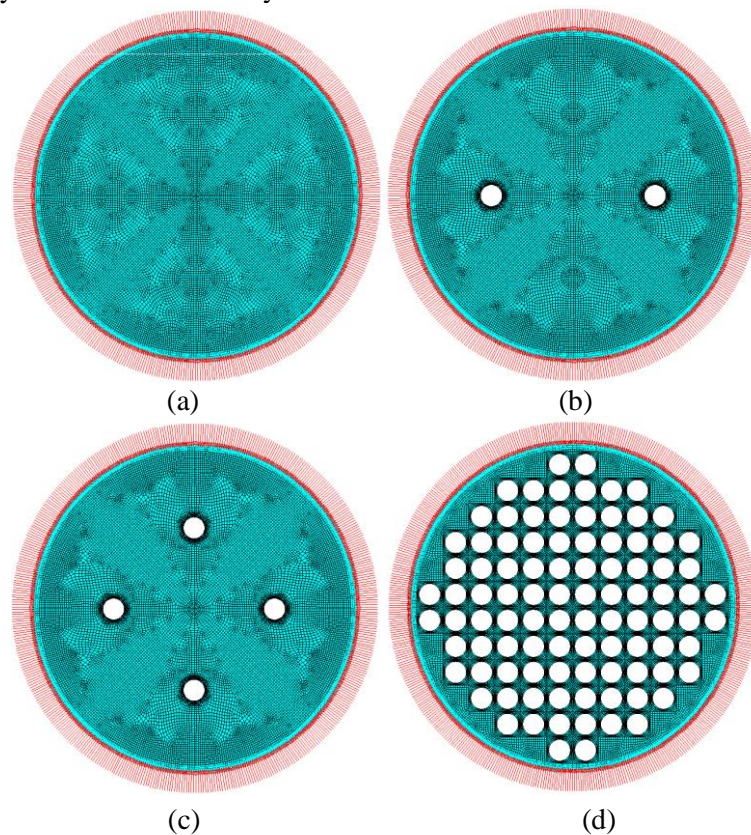
(c)   (d)

Fig.10. Loaden ddiscs with concentrated uniformly distributed load on the contour.

The software Ansys renders the number of loss of stability shapes required for each perforated disc corresponding to the forces that produce them but only the lowest value of the force represents the critical buckling load. From the multitude of cases studied, they are shown in Fig. 11 and in Table 4 when the holes had a radius of 10 mm.

The stability in the non-perforated disc was also studied with the same loading and stress conditions as in fig.10,a to be able to make a comparison with the stability in the perforated disk and calculate the value of the safety factor.

For the full disc, simply supported on the contour, the buckling safety factor for which the calculation was performed, it results [3]. [4]:

$$c = \frac{p_{cr}}{p_\ell} = \frac{2.05^2 \dfrac{D}{R^2}}{\dfrac{F}{2\pi R}} = 2\pi 2.05^2 \frac{D}{FR} = 26.4051 \frac{D}{FR}.$$

For the solid disk, the value of the buckling safety factor c = 54.78 results. Using the FEM-finite element method, the value of the FACT buckling safety factor c = 54.457 was obtained, a result very close to the one obtained analytically.

By running the software, the value of critical loads andof the fact buckling safety was obtained for each studied case. Some of the results obtained by using the finite element method are listed in tables 4, 5 and 6. In fig. 11 are represented fundamental modes of instability for models in Fig. 10 obtained using FEA for r = 10 mm and F = 1000 N.

Table 4. Stability calculations results for discs.

Disc	Disc area [mm^2]	Critical load [N]	Safety factor [-]
Full	70685	54457	54.457
With 2 holes	70057	52796	52.796
With 4 holes	69429	51227	51.227
With 96 holes	40526	16934	16.234

Table 5. Stability calculations results for the perforated disk by four holes

Hole radius [mm]	Disc area [mm^2]	Critical load [N]	Safety factor [-]
5	70371	53608	53.608
10	69429	51227	51.227
20	65659	43540	43.540
30	59376	34600	34.600
40	50579	26100	26.100
50	39269	18920	18.920

Table 6. Stability calculation results for the perforated disc by 96 holes

Hole radius [mm]	Disc area [mm^2]	Critical load [N]	Safety factor [-]
3	67937	48160	48.16
4	65827	44440	44.44
6	59798	35170	35.17
8	51358	25730	25.73
10	40506	16920	16.92
11	34175	12740	12.74

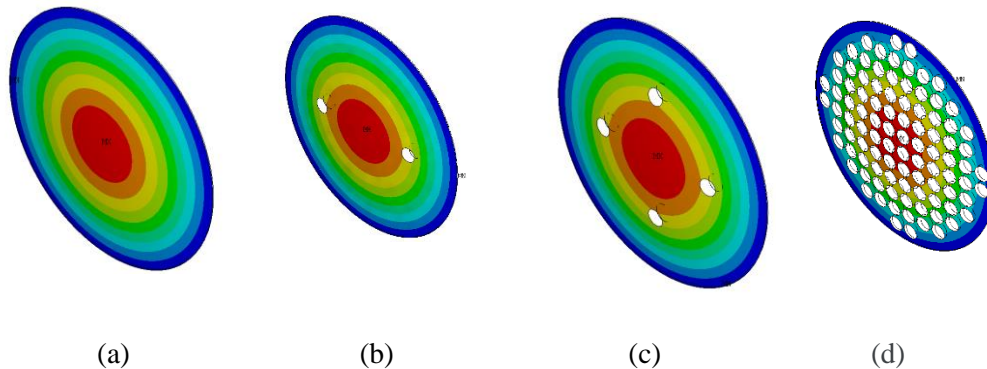|			
(a)	(b)	(c)	(d)

Fig. 11. Fundamental modes of instability for models in Fig. 10 obtained using FEA for $r = 10$ mm and $F = 1000$ N

6. Conclusions

From the research carried out on the stability of perforated discs subjected to compression, several conclusions can be drawn:

 * the method of applying the load significantly influences the stability of the discs. Thus, for the same disc, the critical buckling load and the buckling safety factor increase and therefore the stability of the discs increases if the compression load is transmitted uniformly along their contour,

 * the stiffness of the discs directly influences the stability of the discs. If the effective area of the discs decreases, then the value of the critical buckling load and the buckling safety factor also decrease. For example the disc with 96 holes for the same value of compression force, the value of critical buckling force is almost three times lower than the same non-perforated disc

 * the value of the critical buckling load decreases with the increase of the radius of the holes in the disk with the same value and mode of application of the compression forces.

References

[1] Warren C., Young, *Roark's Formulas for Stress&Strain*, New York, Mc Graw Hill, Inc.
[2] Buzdugan Gh., *Rezistenţa materialelor*, București, Editura Academiei Române, 1986.
[3] Timoshenko S., Gere J., *Teoria stabilităţii elastice*, București, Editura Tehnică, 1967.
[4] Timoshenko S., Woinowsky K., *Teoria plăcilor plane şi curbe*, București, Editura Tehnică, 1968.
[5] Zienkiewicz O.C., *La méthode des éléments finis. Appliquée a l'art de lţingenieur*, Paris, New York, Groupe Mc Graw-Hill.
[6] Sorohan Șt., *Elemente finite în ingineria mecanică*, București, Editura Politehnica Press, 2015.
[7] Atanasiu C., Sorohan Șt., *Stress state in perforated discs*, J Eng. Sci. and Innovation, **8**, 3, 2023, p. 227-238.